

Spin injection from (Ga,Mn)As into InAs quantum dots

Y. Chye, M. E. White, E. Johnston-Halperin, B. D. Gerardot, D. D. Awschalom, and P. M. Petroff
 Center for Spintronics and Quantum Computation University of California, Santa Barbara, California 93106
 (Received 11 July 2002; published 19 November 2002)

Using a spin light emitting diode (spin-LED) we study the injection of spin-polarized holes and electrons from a (Ga,Mn)As epitaxial film into self-assembled InAs quantum dots (QDs). The electroluminescence polarization, integrated over the QD ensemble, is $\sim 1\%$ for both carrier types, consistent with quantum well (QW) spin-LEDs. However, spectrally resolved measurements reveal a monotonic decrease in polarization with increasing energy for hole injection, while no spectral dependence is observed for electron injection. This is in contrast to previous measurements of QW based structures.

DOI: 10.1103/PhysRevB.66.201301

PACS number(s): 72.25.Dc, 72.25.Hg, 75.50.Pp, 73.63.Kv

In recent years, several proposals have been suggested which utilize spin in a quantum dot (QD) as a quantum bit (q-bit).¹ These proposals have found support in the measurement of long spin coherence times for resonantly photoexcited carriers,² and efficient spin relaxation for nonresonant excitation.³ While these optical measurements are promising, it may also prove useful both for issues of scalability and control to *electrically* inject spin-polarized carriers into QDs. In addition, since understanding spin-polarized currents is important for the future development of a spin-based electronics (spintronics),⁴ understanding spin relaxation processes under a variety of conditions is essential. Previous studies have demonstrated electrical injection into quantum wells (QWs) using ferromagnetic semiconductors,^{5–8} ferromagnetic metals,⁹ and paramagnetic semiconductors¹⁰ as spin aligners, suggesting a promising route to achieving this injection. Here we present measurements of a (Ga,Mn)As-based spin light emitting diode (spin-LED) which has been adapted from these previous studies by substituting self-assembled InAs QDs for the QW active region. We have found that the electroluminescence (EL) circular polarization is consistent with the range of values obtained from the QW spin-LEDs for both hole^{5,6} and electron^{7,8} spin injection. In addition, our studies show that hole spin injection is sensitive to variations in QD size and/or material composition, while electron spin injection appears insensitive to these effects.

First, we study hole spin injection into QDs using a standard *p-i-n* LED. A sample schematic can be seen in Fig. 1(a) with the following details: 300 nm p^+ -doped (Ga,Mn)As/30 nm GaAs/InAs QD layer/50 nm GaAs/ n -doped GaAs:Si ($5 \times 10^{18} \text{ cm}^{-3}$). Here the designation p^+ -doped for the (Ga,Mn)As layer refers to the native hole doping found in this alloy, typically $\sim 1 \times 10^{19} \text{ cm}^{-3}$ for these Mn levels.¹¹ The (Ga,Mn)As layer acts as a hole spin polarizer.^{5,6} A nonmagnetic *p-i-n* LED control sample in which the (Ga,Mn)As layer is replaced by a GaAs:Be layer ($1 \times 10^{19} \text{ cm}^{-3}$) is also measured. Second, we study electron spin injection by employing a Zener diode/*n-i-p* LED device^{7,8} (ZD LED) with the following structure: 300 nm p^+ -doped (Ga,Mn)As/10 nm n^+ -doped GaAs:Si ($2 \times 10^{19} \text{ cm}^{-3}$)/200 nm n -doped GaAs:Si ($5 \times 10^{16} \text{ cm}^{-3}$)/30 nm GaAs/InAs QD layer/50 nm GaAs/ p -doped GaAs:Be ($5 \times 10^{18} \text{ cm}^{-3}$). A sample schematic and its energy band diagram for this structure can be seen in Fig. 1(b), where the

(Ga,Mn)As layer and the n^+ -doped GaAs:Si layer form the Zener diode. When a reverse bias is applied across this junction, the *electrons* from the (Ga,Mn)As valence band tunnel across the bandgap into the conduction band of the n -GaAs and subsequently flow into the QDs.

The devices are grown by molecular-beam epitaxy (MBE) on semi-insulating GaAs (100) substrates. To ensure high luminescence quality for the QDs, the QD layer and the doped/undoped GaAs layers are grown in an MBE chamber optimized for optoelectronic materials. All GaAs layers are grown at 580 °C except the QD layer, which is grown at 540 °C. The QDs are grown using the partially covered island technique¹² to tune the ground-state luminescence to $\sim 1.25 \text{ eV}$. An amorphous As protective cap is deposited at room temperature before transfer into a second MBE chamber optimized for low-temperature (Ga,Mn)As regrowth. In

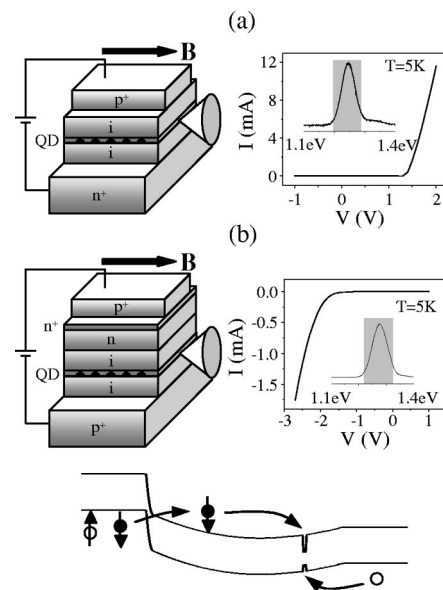


FIG. 1. (a) and (b) The schematic structures, I - V characteristics, and EL spectra for the standard *p-i-n* LED and ZD LED, respectively. An in-plane magnetic field is applied along [110] and the EL is collected from the (110) cleaved edge. The I - V and EL spectra are taken at $T=5 \text{ K}$. The shaded areas in the spectra indicate the region of polarization integration over the QDs ensemble. Bottom is the schematic of the tunneling process for the ZD LED.

this chamber, the As cap is evaporated by annealing at $\sim 350^\circ\text{C}$ under an As flux before the (Ga,Mn)As is grown at 260°C . The Mn composition is 5.1% for the *p-i-n* LED (5.2% for the ZD LED) as measured by MnAs reflection high-energy electron diffraction oscillations.¹³ Finally, a control sample with the (Ga, Mn)As layer replaced by a *p*-GaAs layer is also grown.

Devices are fabricated using standard photolithography and wet chemical etching resulting in a wedding-cake structure with a mesa stripe $200\ \mu\text{m}$ wide on top of a mesa stripe $400\ \mu\text{m}$ wide. A $100\ \mu\text{m}$ -wide Ti:Au stripe is deposited onto the top mesa for electrical contact. The mesa stripe is oriented along [110] and the device is cleaved along $[\bar{1}10]$ on both ends to facilitate edge emission along [110]. Measurements are done in an optical cryostat (at temperatures $T = 3\text{--}300\ \text{K}$) with a hand-wound electromagnet that generates a magnetic field parallel to the LED emission. Figures 1(a) and 1(b) show the *I-V* characteristics with turn-on voltages of about 1.25 and 1.7 V for the *p-i-n* LED and the ZD LED, respectively.

The EL spectra of both LEDs, taken at 5 K, are shown in the insets in Figs. 1(a) and 1(b) for the *p-i-n* and the ZD LEDs, respectively. The emission peak is centered at $\sim 1.25\ \text{eV}$ for the *p-i-n* LED and $\sim 1.28\ \text{eV}$ for the ZD LED. They both have a full width at half maximum of approximately 50 meV due to the inhomogeneous size distribution of the QDs.¹⁴ The EL collected from the cleaved edge passes through a broadband quarter wave plate with retardation accuracy of $\pm\lambda/100$ over a bandwidth from 900 nm (1.38 eV) to 1270 nm (0.98 eV). The quarter wave plate transforms the left and right circularly polarized luminescence (LCP and RCP) into vertical and horizontal linear polarizations, respectively. This linearly polarized light is then analyzed using a linear polarizer and spectrally resolved using a Si-based liquid-nitrogen-cooled charge coupled device attached to a spectrometer. The intensities of the LCP and RCP light are measured and the polarization, defined as $P = (I^{\text{LCP}} - I^{\text{RCP}})/(I^{\text{LCP}} + I^{\text{RCP}})$, is calculated. Here I^{LCP} and I^{RCP} are the integrated intensities of LCP and RCP luminescence, respectively, with the range of integration as shown by the shaded areas in the spectra in Figs. 1(a) and 1(b).

In Fig. 2(a), we show the hysteresis plot of the polarization of the EL (triangles) for the *p-i-n* LED measured at $T = 5\ \text{K}$ and at a voltage bias of 1.7 V. Note that a field-independent background of approximately 3% has been subtracted from the polarization to facilitate comparison with magnetization data. The magnetization hysteresis of the (Ga,Mn)As layer, as measured on an unprocessed sample with a superconducting quantum interference device (SQUID) magnetometer, is also shown in Fig. 2(a) (dashed line), and is consistent with the measured polarization. The discrepancy in the coercive field between the polarization and the magnetization may arise from the fact that the coercivity is an extrinsic property; as such it can be modified by demagnetizing fields, domain wall pinning, etc. which may be dependent on the details of the device processing. Additionally the electrical currents present in the polarization measurement may have some impact on the magnetic properties of the (Ga,Mn)As film. Figure 2(b) shows the polar-

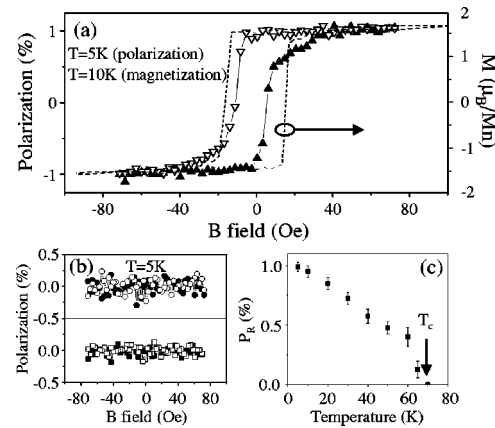


FIG. 2. (a) EL polarization (triangles) hysteresis for the *p-i-n* LED. The dashed line indicates the in-plane (Ga,Mn) As magnetization hysteresis measured with a SQUID magnetometer. (b) No hysteresis is observed for the *p-i-n* LED PL polarization (circles) and the control sample EL polarization (squares) measured in the same geometry. Open symbols denote a down-sweep of the magnetic field and closed symbols denote an up-sweep. Note that a field-independent background polarization has been subtracted. (c) P_R as a function of temperature.

ization of the photoluminescence (PL) (circles) for the *p-i-n* LED excited by a linearly polarized He-Ne laser (633 nm or 1.96 eV) and the EL (squares) for the control sample taken at 5 K using the same geometry. A field-independent background of approximately -1.4% has been subtracted from the PL polarization and -1% from the control sample EL polarization. The absence of field dependence in the PL and control sample EL polarizations excludes artifacts due to luminescence scattering from the dichroic (Ga,Mn)As layer¹⁵ or to strain-induced effects. The remnant polarization (P_R) as a function of temperature is shown in Fig. 2(c), where it is seen to decrease with increasing temperature and vanish at $\sim 70\ \text{K}$. We find a Curie temperature (T_C) from SQUID magnetometry for the (Ga,Mn)As layer of $\sim 70\ \text{K}$, agreeing well with the measured temperature dependence of P_R . These results verify that spin-polarized holes are injected into the QDs.

The EL measurements are also performed for the ZD LED to investigate the injection of spin-polarized electrons into the QDs. The EL polarization hysteresis at $T = 5\ \text{K}$ in Fig. 3(a) shows that electron spin injection is indeed occurring with a remnant polarization at $T = 5\ \text{K}$ of $\sim 1.25\%$. Also shown is the field independent PL polarization (circles) measured in the same geometry. P_R as a function of temperature is shown in Fig. 3(b), again consistent with a T_C of $\sim 70\ \text{K}$.

In attempting to quantitatively correlate the measured optical polarization described above with the free-carrier spin polarization there are a number of distinct stages in the spin transport that must be considered. For convenience, we group these processes into four distinct categories: (1) spin polarization in the (Ga,Mn)As, (2) transport across the (Ga,Mn)As/GaAs heterointerface and through bulk GaAs, (3) injection into the QDs and subsequent energy relaxation, and (4) the efficiency of conversion from carrier spin to optical polarization *via* radiative recombination processes.

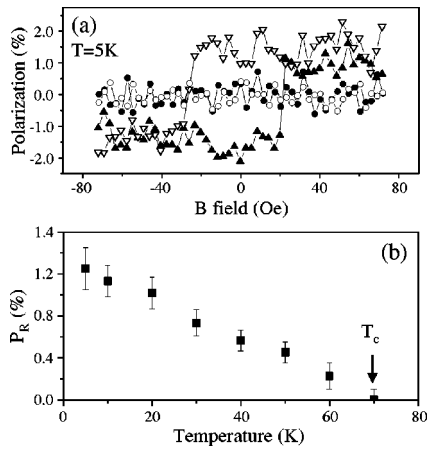


FIG. 3. (a) EL polarization hysteresis (triangles) and PL polarization (circles) for the ZD LED as a function of an in-plane magnetic field. Open symbols denote a down-sweep of the magnetic field and closed symbols an up-sweep. (b) P_R versus temperature for the same device.

While there has been extensive theoretical work addressing the intrinsic spin polarization in (Ga,Mn)As,¹⁶ there is to our knowledge no direct experimental evidence on this issue. We therefore focus the following discussion on the final three processes.

Previous measurements of coherent spin transport in semiconductors have shown efficient electron spin-transfer across a GaAs/ZnSe heterointerface¹⁷ and through bulk n -doped GaAs.¹⁸ Furthermore, measurements on QW spin-LEDs with paramagnetic injection layers¹⁰ have yielded optical polarizations approaching 50% for all electrical electron injection. Taken together these results strongly suggest that scattering during transport is not the limiting factor in the electron-injection measurements. The picture is less clear for the holes as there have been recent reports of anisotropic hole spin transport in QW spin-LEDs,⁶ and a deeper understanding of this process is required before assessing its relative importance. Regarding injection into the QDs, there has also been work with optically pumped QD samples addressing the spin lifetime under nonresonant pumping conditions³ (the conditions most analogous to the situation in this study). Photoluminescence polarizations as high as $\sim 12\%$ were measured when carriers were photo-excited in the GaAs matrix and subsequently relaxed into the QDs before recombining. Assuming optical pumping yields an electron spin polarization of 50% in bulk GaAs,¹⁹ and a 100% conversion efficiency of this spin polarization into optical polarization in the luminescence,²⁰ this yields a minimum spin-injection efficiency of $\sim 25\%$.

Finally, as discussed in detail regarding QW spin-LEDs,⁵⁻⁷ it is important to consider that both heavy and light holes (HH and LH, respectively) are present in the QDs. In other words, it is quite difficult to reconstruct the exact exciton giving rise to the observed polarization without some knowledge of which hole specie is participating in the recombination. For example, both $|+3/2, -1/2\rangle$ and $|+1/2, +1/2\rangle$ excitons will give rise to LCP luminescence upon recombination (where the notation refers to $|\text{hole spin, electron}$

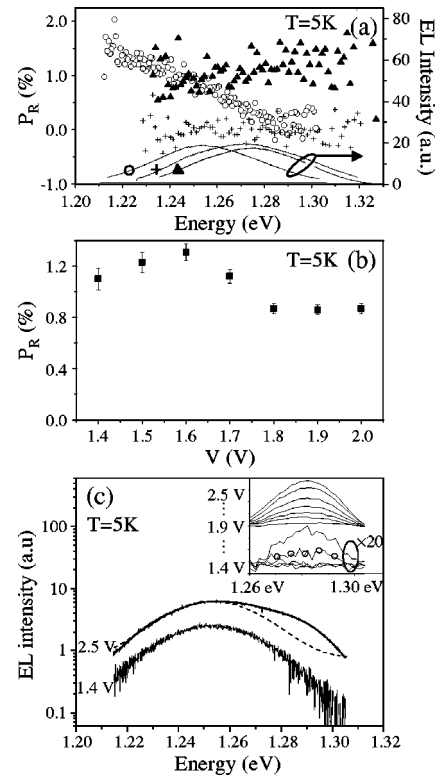


FIG. 4. (a) EL spectra and the spectrally resolved EL P_R versus emission energy for the p - i - n LED (circles), ZD LED (triangles), and control sample (crosses). The center emission peaks are 1.25, 1.28, and 1.27 eV for the p - i - n LED, ZD LED, and control sample, respectively. The measurements are taken at $T=5$ K. (b) P_R for EL emission energy $E=1.25$ eV as a function of applied bias voltage. (c) EL spectra at $V=1.4$ and 2.5 V for the p - i - n LED. Emission from the first QD excited state at $E\sim 1.285$ eV is seen in the spectrum at $V=2.5$ V. The Gaussian fit for the ground state EL peak is also shown (dashed line). Inset shows EL spectra of the first excited state, obtained by subtracting the Gaussian fit to the ground-state peak from the EL spectra. Spectra are shown from $V=1.4$ V to 2.5 V with a 0.1 V increment. The onset of the first excited state is at $V\sim 1.7$ V (line plus circles).

spin) and the sign convention is chosen so that positive corresponds to spin oriented along the direction of propagation of the luminescence).¹⁹ In principle, one should be able to resolve this ambiguity through a calculation of the HH-LH splitting in the QDs due to both strain and quantum confinement. However in practice the strain in this system is complicated by the superposition of the strained QD layer with the strained (Ga,Mn)As layer, making such calculations difficult. In addition, it is unclear whether attempts to disentangle the HH and LH based on symmetry arguments in QW based spin-LEDs (Ref. 7) are applicable in this QD-based device. It is important to note that these limitations apply to both hole and electron spin injection.

The QD system consists of an ensemble of dots with different sizes and material compositions²¹ producing a broad luminescence spectrum. Analysis of P_R as a function of emission energy may therefore yield insights into the spin injection efficiency in different kinds of QDs. To obtain the spectrally resolved P_R , we calculate P_R for each emission

energy measured in the EL spectra. Figure 4(a) shows EL spectra and P_R versus emission energy for the p - i - n LED (circles), ZD LED (triangles), and control sample (crosses). For the p - i - n LED, P_R decreases with increasing EL emission energy (independent of the applied voltage). This trend disappears when the sample temperature is raised above T_C . On the other hand, the spectrally resolved polarizations of the ZD LED and control sample are found to be constant across the spectrum [Fig. 4(a), triangles and crosses, respectively], excluding artifacts associated with the instruments or the background polarization. The electron and hole trajectories are almost identical in both types of QD spin LED devices and therefore device geometry should have minimal effects on the EL path. The results of the ZD LED and control sample therefore exclude a wavelength dependent dichroic scattering effect when the EL propagates in the p - i - n LED as the origin of the wavelength-dependent polarization signal. This suggests that the variation is likely associated with changes in QD size and/or material composition.

A possible explanation for this behavior is that as the QD potential becomes shallower, i.e., for decreasing In content or smaller dot radius/height, the carriers are less confined. Under these conditions, processes such as up-conversion²² and increased interaction between polarized holes within the QDs and the carriers in the wetting layer are possible and may play a role in spin scattering. The fact that the measured P_R versus emission energy for the ZD LED is almost constant across the spectrum [Fig. 4(a), triangles] would then suggest that electrons are less sensitive than holes to changes in the size or material composition of the QDs. Other potential explanations for this difference between the conduction

and valence band include differing spin lifetimes, residual doping, spin-orbit interactions, etc.

For the p - i - n LED, we also observe a variation in P_R as a function of the applied voltage for emission energies ranging from 1.225 to 1.275 eV. A representative scan taken at an energy of 1.25 eV (the center of the QD ensemble ground state) can be seen in Fig. 4(b). The decrease of polarization takes place at roughly the same voltages where excited state EL is first observed [~ 1.7 V, Fig. 4(c)]. This is consistent with previous results from optically pumped QDs that have shown both a shorter spin-lifetime for the excited state and an overall decrease in polarization with the onset of excited-state luminescence.³ Possible explanations for this behavior include partial hybridization of the excited state with wetting layer states or carrier-carrier scattering within the QD.

To conclude, we have successfully demonstrated the injection of spin-polarized holes and electrons into QDs from a (Ga,Mn)As epitaxial layer. The measured EL polarization for QD spin-LEDs is consistent with the range of values measured in QW spin-LEDs.⁵⁻⁸ Finally, in contrast to measurements of QW-based devices, spectrally resolving the optical polarization arising from the injection of spin-polarized holes into InAs QDs reveals a sensitivity to the QD size and/or material composition. This sensitivity is not observed for spin-polarized electron injection.

We acknowledge R. Kawakami, J. English, I. Meinel, and L. Kinder for technical assistance and advice. E. J. H. would like to thank D. K. Young for stimulating discussions. This project is supported by DARPA/ONR N00014-99-1-1096. M. W. is supported by a NSF-IGERT grant.

-
- ¹D. Loss and D. P. DiVincenzo, Phys. Rev. A **57**, 120 (1998); G. Burkard, *et al.*, Phys. Rev. B **59**, 2070 (1999); A. Imamoglu *et al.*, Phys. Rev. Lett. **83**, 4204 (1999).
- ²J. A. Gupta *et al.*, Phys. Rev. B **59**, R10 421 (1999); M. Paillard *et al.*, Phys. Rev. Lett. **86**, 1634 (2001).
- ³R. J. Epstein *et al.*, Appl. Phys. Lett. **78**, 733 (2001).
- ⁴G. A. Prinz, Phys. Today **48**, 58 (1995); G. A. Prinz, Science **282**, 1660 (1998); S. A. Wolf *et al.*, *ibid.* **294**, 1488 (2001).
- ⁵Y. Ohno *et al.*, Nature (London) **402**, 790 (1999).
- ⁶D. K. Young *et al.*, Appl. Phys. Lett. **80**, 1598 (2002).
- ⁷E. Johnston-Halperin *et al.*, Phys. Rev. B **65**, 041306 (2002).
- ⁸M. Kohda *et al.*, Jpn. J. Appl. Phys., Part 2 **40**, L1274 (2001).
- ⁹H. J. Zhu *et al.*, Phys. Rev. Lett. **87**, 016601 (2001).
- ¹⁰R. Fiederling *et al.*, Nature (London) **402**, 787 (1999); B. T. Jonker *et al.*, Phys. Rev. B **62**, 8180 (2000).
- ¹¹H. Shimizu *et al.*, Appl. Phys. Lett. **74**, 398 (1999).
- ¹²J. M. Garcia *et al.*, Appl. Phys. Lett. **72**, 3172 (1998).
- ¹³R. K. Kawakami *et al.*, Appl. Phys. Lett. **77**, 2379 (2000), and references therein.
- ¹⁴D. Leonard *et al.*, Appl. Phys. Lett. **63**, 3203 (1993).
- ¹⁵B. Beschoten *et al.*, Phys. Rev. Lett. **83**, 3073 (1999).
- ¹⁶H. Akai, Phys. Rev. Lett. **81**, 3002 (1998); S. Sanvito, G. Theurich, and N. A. Hill, J. Supercond. **15**, 85 (2002), and references therein.
- ¹⁷I. Malajovich *et al.*, Phys. Rev. Lett. **84**, 1015 (2000).
- ¹⁸J. M. Kikkawa and D. D. Awschalom, Phys. Rev. Lett. **80**, 4313 (1998).
- ¹⁹M. I. Dyakonov and V. I. Perel, in *Optical Orientation*, edited by F. Meir and B. P. Zakharchenya (North-Holland, New York, 1984).
- ²⁰The actual conversion efficiency is unknown and could be much lower due to heavy-hole light-hole mixing (see following paragraph). However, this value provides a *minimum* relaxation efficiency.
- ²¹I. Kegel *et al.*, Phys. Rev. Lett. **85**, 1694 (2000).
- ²²P. P. Paskov *et al.*, Appl. Phys. Lett. **77**, 812 (2000).